MRS Advances © 2018 Materials Research Society
DOI: 10.1557/adv.2018.446

Fungi-Derived Pigments for Sustainable Organic (Opto)Electronics

Gregory Giesbers, Jonathan Van Schenck, Sarath Vega Gutierrez, Sara Robinson, Oksana Ostroverkhova

Oregon State University, Corvallis, OR, United States

ABSTRACT

We present on the optical and electronic properties of a fungi-derived pigment xylindein for potential use in (opto)electronic applications. Optical absorption spectra in solutions of various concentrations and in film are compared and are consistent with aggregate formation in concentrated solutions and films. In order to improve film morphology obtained by solution deposition techniques, an amorphous polymer PMMA was introduced to xylindein to form xylindein:PMMA blends. Current-voltage characteristics and hole mobilities extracted from space-charge limited currents were found to be comparable between pristine xylindein and xylindein:PMMA films. Side by side comparison of the photoresponse of pristine xylindein and xylindein:PMMA films at 633 nm revealed an increase in the photosensitivity in xylindein:PMMA films due to the improved morphology favouring enhanced charge generation.

INTRODUCTION

Organic semiconductor materials are of interest for use in optoelectronic applications due to their low cost, solution processability, and tunable properties. Among various classes of organic materials, over the past decade there has been a growing research effort focusing on green chemistry and on sustainable, natural product-derived materials for organic electronics.[1],[2] Successful examples of the latter include indigo and Tyrian purple dyes, isoindigo, and diketopyrrolopyrrole derivatives which have been used in ambipolar organic field-effect transistors (OFETs) and donor-acceptor (D/A) solar cells.[3] Fungi-derived pigments are a naturally sourced, sustainable class of materials that are currently unexplored as organic semiconductor materials. We seek to explore this novel class of natural product-derived (opto)electronic materials, in this paper focusing on a fungi-derived pigment xylindein, which is secreted from the fungi *Chlorociboria aeruginosa* and *Chlorociboria aeruginascens*. Wood stained with xylindein has been utilized by humans in decorative wood products since the 1400s; that the pigment remains blue-green in intarsia artwork aged 500+ years is a testament to its environmental durability.[4] However, optical and (opto)electronic properties of this pigment have not yet been characterized, and our initial efforts towards understanding these properties in xylindein and other fungi-derived pigments are presented here.

EXPERIMENTAL

Xylindein Culturing and Extraction

Xylindein is a spalting pigment produced by the wood-eating fungi, *Chlorociboria aeruginosa* and *Chlorociboria aeruginascens* (Fig 1(a)). We have developed a method for the reliable culturing, extraction, and purification of xylindein as described in our previous publications.[5]–[7] Briefly, *C. aeruginosa* is cultured on 10 cm plates in a 2% malt, 1.5% agar in water solution (Fig. 1(b)). Mature fungal materials are then transferred to bioreactors containing 2% malt in water. As the fungal material secretes xylindein into the liquid media, some of the liquid is regularly collected and purified to yield the pigment (Fig. 1(c-e)).[7]

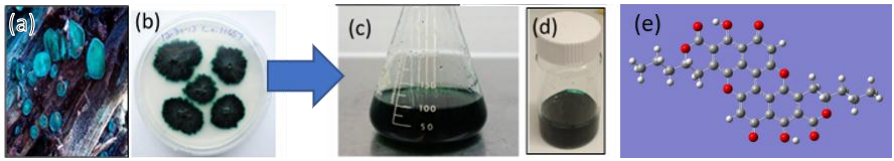

Figure 1. (a) Fruiting bodies of *C. aeruginosa*. (b) *C. aeruginosa* cultured on solid media. (c) *C. aeruginosa* secretes xylindein in liquid culture. (d) Xylindein purified from liquid cultures. (e) Molecular structure of xylindein.

Materials

The core structure of the xylindein molecule (Fig. 1(e)) is *peri*-xanthenoxanthene (PXX), derivatives of which were shown to exhibit hole mobilities of up to 0.9 $cm^2/(Vs)$[8],[9] and explored by Sony for use in OFET-driven displays due to their unprecedented stability.[10] Promising electronic characteristics and stability, which has been previously demonstrated through prolonged exposure to UV light, electrical stress, and thermal stress,[11] motivates the choice of xylindein for this study. When deposited from solution, xylindein forms a highly disordered porous, amorphous solid which may be disadvantageous for electronic properties favourable for device applications, as well as their reproducibility. To gain improvement of morphology in the xylindein thin-film devices and enhance the quality of solution-deposited thin films, we introduced a transparent non-conductive polymer, poly(methyl methacrylate) (PMMA) as a host matrix and explored properties of xylindein:PMMA blends side-by-side with pristine xylindein films.[12]

Sample preparation

Solid flakes of purified xylindein were mixed into chlorobenzene and tetrahydrofuran (THF) to form solutions of various concentrations. THF solutions in the 8-180 µM range of concentrations were used for solution absorption measurements, and 10 mM and 25 mM chlorobenzene solutions were used for depositing films. For xylindein:PMMA samples, a 180 mM solution of PMMA in chlorobenzene was prepared and 10 µL of this solution was mixed with 180 µL of 10 mM xylindein solution to yield a composite solution containing xylindein and PMMA at a 1:1 molar ratio. All solutions were sonicated for at least 30 minutes. Pristine xylindein and xylindein:PMMA films were obtained by drop-casting corresponding solutions at room temperature onto interdigitated Au/Cr electrodes deposited on a glass substrate with a gap of 25µm.[13] Prior to film deposition, the substrates were sonicated in an acetone bath and rinsed with deionized water to eliminate foreign contaminants. Pristine xylindein films were studied using the

x-ray diffraction (XRD) and scanning electron microscopy (SEM). The XRD confirmed an amorphous nature of films, and the SEM revealed porous structure as shown in Fig. 2.

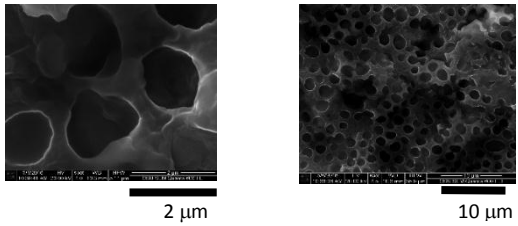

Figure 2. SEM images of drop-cast pristine xylindein films showing their porous structure.

Measurement Procedures

Optical absorption was taken at room temperature in air using an Ocean Optics USB-2000 spectrometer and an LS-1 tungsten halogen lamp. Electrical measurements were performed using a Keithley 237 source-measure unit. Current-voltage (I-V) characteristics were measured with a sweep in voltage increasing in 1 V increments from 1 V to 300 V and measuring the current output in a dark room at room temperature. Effective charge carrier (hole) mobilities were extracted from space-charge limited currents (SCLCs) using thin-film and half-space approximations as detailed in Ref. [13]. Current in the presence of a 633 nm 1.3 mW illumination from a HeNe laser was measured at a constant voltage (100 V) as follows. Voltage was applied, and dark current was recorded for 5 seconds. Then, the light was turned on with a shutter and the current under illumination was measured as a function of time. The photocurrent was calculated as the difference between the two, and the photosensitivity was obtained by dividing the photocurrent by the dark current. In order to make comparisons of the photosensitivity between the samples with different optical densities, photosensitivity per absorbed photon was calculated as the photosensitivity divided by $(1\text{-}10^{\text{-OD}})$, where OD is the optical density obtained from absorption spectra of films at 633 nm.

RESULTS AND DISCUSSION

Optical Properties

Optical absorption spectra of xylindein in solutions of various concentrations, in pristine film, and in xylindein:PMMA film are shown in Figure 3. The absorption spectrum of xylindein in all solutions features a dominant peak at ~670 nm and a structure consistent with vibronic progression due to exciton coupling to C-C stretching modes similar to that observed in many organic semiconductor molecules such as acenes or acene-thiophenes.[14] The xylindein and xylindein:PMMA film absorption spectra (Fig. 3(b)) exhibit less pronounced vibronic progression features as compared to those in solution due to disorder-induced peak broadening. Additionally, they exhibit a new band at ~720 nm. The 720 nm band also occurs in solutions at higher concentrations (Fig. 3(a)), which suggests that it is due to aggregate formation.[12] The nature of these aggregates, which involve an interplay between intermolecular hydrogen bonding[15] and π–π stacking of xylindein molecules, is currently unknown and needs further investigation. The wide range of absorption in films extending to the near-infrared (IR) wavelength region obtained in films is beneficial for (opto)electronic devices such as D/A bulk heterojunction (BHJ) solar cells and applications specifically relying on the optical response in the near-IR.[16]

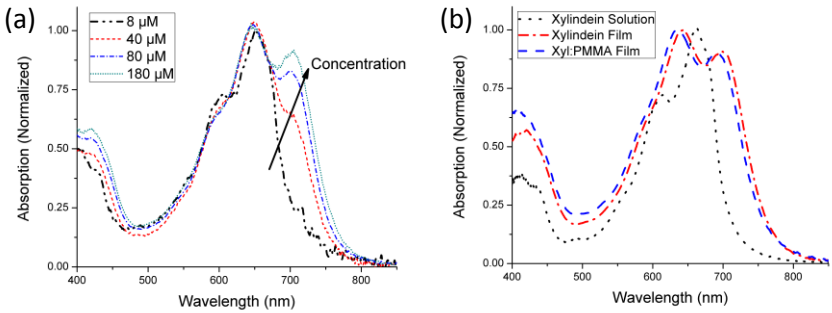

Figure 3. Normalized absorption spectra for (a) 8-180 μM xylindein in THF solutions and (b) drop-cast films of xylindein and xylindein:PMMA (1:1).

Electrical Properties

Xylindein films have been previously shown to exhibit an effective charge carrier (hole) mobility of up to 0.53 $cm^2/(Vs)$ despite un-optimized deposition conditions and poor morphology.[11] Given that pristine xylindein tends to form non-uniform films with an amorphous porous structure with current deposition techniques, an important step to the use of xylindein in (opto)electronic devices is to understand how film deposition method affects the performance and to improve film morphology.[17] We found that mobility obtained from drop-cast xylindein films varies by several orders of magnitude depending on the concentration of the solution used in film preparation and sample area. Solutions with higher xylindein concentrations produce thicker films, and small sample areas facilitate a better surface coverage; both yield higher values of mobilities.[11] The solution concentrations and preparation method reported here yielded xylindein films with hole mobilities on the order of 10^{-3} $cm^2/(Vs)$. One strategy to improve film quality and enhance solution processability of small-molecule organic semiconductors has been to create blends of the organic semiconductor molecule with an amorphous polymer.[18] This strategy has proved successful for organic semiconductor molecules with a strong tendency to crystallize (such as anthradithiophene (ADT) derivatives), as enhanced mobility in ADT:polymer blends was obtained (as compared to that in pristine ADT films) due to reduced charge trap densities.[18] Aiming to achieve a similar goal, we introduced PMMA as a polymer host matrix, to fill in the pores of the native xylindein and create more uniform films.[12] Given the non-conductive property of PMMA, it is then important to determine the possible trade-off between the film quality and its electrical characteristics which we discuss next.

Side by side comparison of I-V curves of xylindein and xylindein:PMMA films obtained using the same xylindein solutions for deposition show similar electrical characteristics (Fig. 4(a)). Both films experience a shift to the SCLC regime, where the I-V curve switches from linear to quadratic, at ~120 V. For the samples in Fig. 4(a), the effective charge carrier (hole) mobilities extracted from the slopes of a linear fit to a plot of current versus the square of voltage in the SCLC regime (inset of Fig. 4(a)) yielded 4.2 x 10^{-3} (9.5 x 10^{-3}) $cm^2/(Vs)$ and 4.6 x 10^{-3} (1.0 x 10^{-2}) $cm^2/(Vs)$ in pristine xylindein and xylindein:PMMA samples, respectively, in thin-film (half-space) approximations.[13] Similarity of the mobility values obtained in pristine xylindein and xylindein:PMMA films is promising for creating uniform thin-film devices with enhanced processability based on xylindein:polymer blends.

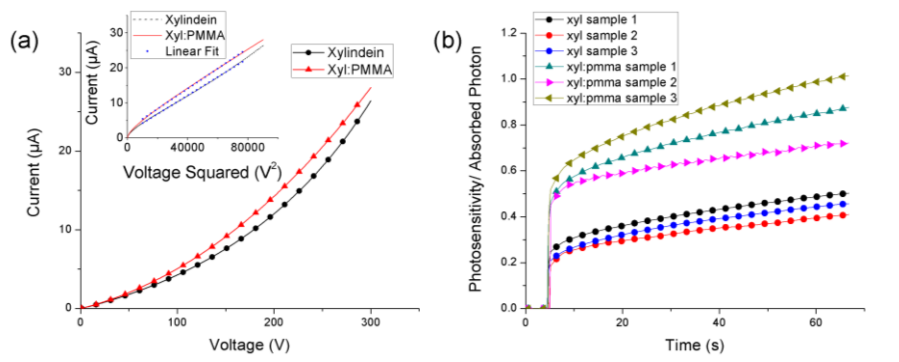

Figure 4. (a) Current-voltage characteristics from a 1-300V voltage sweep for a pristine xylindein film and a xylindein:PMMA (1:1) film. Inset shows the same curves plotted against the square in voltage with a linear fit in the SCLC regime from which effective hole mobilities are obtained. (b) Photosensitivity per absorbed photon for three pristine xylindein films and three xylindein:PMMA films on interdigitated Au/Cr electrodes obtained at an applied voltage of 100 V and 633 nm 1.3 mW laser illumination initiated at t=5 seconds.

Furthermore, the xylindein:PMMA films exhibited a stronger photoresponse in the visible spectral range as compared to pristine xylindein films (Fig. 4(b)). Comparing three xylindein films with three xylindein:PMMA films made from the same xylindein solution with identical processes, we observed a factor of ~2 increase in the photosensitivity per absorbed photon in the xylindein:PMMA films. Since PMMA is transparent in the visible wavelength range, it does not directly contribute to the enhanced photosensitivity at 633 nm observed here. Given that charge carrier mobilities in these xylindein and xylindein:PMMA samples are comparable, the observed increase in photosensitivity indicates an improved charge photogeneration efficiency. This suggests that the film morphology achieved in xylindein:PMMA blends favours a reduced efficiency of geminate recombination as compared to that in pristine xylindein films. Establishment of the exact mechanism behind this observation and its potential utility for polymer:xylindein D/A BHJ solar cells will be a subject of our future investigation.

CONCLUSION

Optical absorption measurements reveal aggregate formation, manifested via an appearance of a ~720 nm absorption band, red-shifted from the spectra of dilute solutions, in solutions with higher concentrations and in films as compared to dilute solutions. The nature of such aggregates that are created by an interplay of intermolecular hydrogen bonding and π–π stacking requires further investigation. Addition of PMMA to pristine xylindein is a promising route to improve the film morphology and solution processability without detriment to the electrical characteristics of the film. Charge carrier (hole) mobilities on the order of 10^{-3} $cm^2/(Vs)$ were obtained both from pristine xylindein and xylindein:PMMA films. A factor of ~2 improvement in photosensitivity was observed in xylindein:PMMA films as compared to pristine xylindein films, due to an enhanced charge generation efficiency caused by an improved

film morphology. The mechanism of this enhancement and how it could be used in (opto)electronic thin-film devices incorporating xylindein will be explored in our future work.

ACKNOWLEDGEMENTS

This work was supported by the National Science Foundation (NSF-CBET 1705099). We thank A. Quinn, R. Harrison, J. Rath, Dr. G. Weber, Dr. B. Johnson, and Prof. V. Remcho for their contributions to the initial stages of this work.

References

1. M. Irimia-Vladu, E.D. Glowacki, N.S. Sariciftci, and S. Bauer, in *Small Org. Mol. Surfaces* (2013), pp. 295–318.
2. A. Marrocchi, A. Facchetti, D. Lanari, C. Petrucci, and L. Vaccaro, Energy Environ. Sci. **9**, 763 (2016).
3. O. Ostroverkhova, Chem. Rev. **116**, 13279 (2016).
4. S. Robinson, Am. Sci. **102**, 206 (2014).
5. S.C. Robinson, E. Hinsch, and G. Weber, Color. Technol. **130**, 221 (2014).
6. G. Weber, H.L. Chen, E. Hinsch, S. Freitas, and S. Robinson, Color. Technol. **130**, 445 (2014).
7. S.C. Robinson, D. Tudor, H. Snider, and P.A. Cooper, AMB Express **2**, 15 (2012).
8. J. Mei, Y. Diao, A.L. Appleton, L. Fang, and Z. Bao, J. Am. Chem. Soc. **135**, 6724 (2013).
9. N. Kobayashi, M. Sasaki, and K. Nomoto, Chem. Mater. **21**, 552 (2009).
10. N. Yoneya, H. Ono, Y. Ishii, K. Himori, N. Hirai, H. Abe, A. Yumoto, N. Kobayashi, and K. Nomoto, J. Soc. Inf. Disp. **20**, 143 (2012).
11. R. Harrison, A. Quinn, G. Weber, B. Johnson, J. Rath, V. Remcho, S. Robinson, and O. Ostroverkhova, in *SPIE* (2017), p. 101101U.
12. W.E.B. Shepherd, A.D. Platt, D. Hofer, O. Ostroverkhova, M. Loth, and J.E. Anthony, Appl. Phys. Lett. **97**, 163303 (2010).
13. J. Day, A.D. Platt, S. Subramanian, J.E. Anthony, and O. Ostroverkhova, J. Appl. Phys. **105**, 1 (2009).
14. A. Platt, M. Kendrick, M. Loth, J. Anthony, and O. Ostroverkhova, Phys. Rev. B **84**, 235209 (2011).
15. M. Sytnyk, E.D. Głowacki, S. Yakunin, G. Voss, W. Schöfberger, D. Kriegner, J. Stangl, R. Trotta, C. Gollner, S. Tollabimazraehno, G. Romanazzi, Z. Bozkurt, M. Havlicek, N.S. Sariciftci, and W. Heiss, J. Am. Chem. Soc. **136**, 16522 (2014).
16. L. Dou, J. You, Z. Hong, Z. Xu, G. Li, R.A. Street, and Y. Yang, Adv. Mater. **25**, 6642 (2013).
17. J. Bisquert, J. Phys. Chem. Lett. **3**, 1515 (2012).
18. S. Hunter, J. Chen, and T.D. Anthopoulos, Adv. Funct. Mater. **24**, 5969 (2014).